An Advanced Lithium-Ion Sulfur Battery for High Energy Storage

Marco Agostini, Bruno Scrosati, and Jusef Hassoun**

A lithium-ion battery is reported using a sulfur–carbon composite cathode, a graphite anode, and a dimethoxyethane-dioxolane-lithium bis-(trifluoromethanesulfonyl)imide (DOL-DME-LiTFSI) electrolyte advantageously added by lithium nitrate ($LiNO_3$) and a selected polysulfide (Li_2S_8). The suppressed sulfur dissolution, due to the Li_2S_8 buffer action, as well as reduced shuttle reactions by the film-forming properties of the $LiNO_3$ positively affect the lithium-ion cell behavior in terms of delivered capacity, coulombic efficiency, and cycle life. The lithium–sulfur cell shows a stable capacity of 750 mAh g^{-1} for over 200 cycles with an enhanced cycling efficiency. Furthermore, the full lithium-ion sulfur battery using a graphite-based anode shows a working voltage of about 2 V and delivers a stable capacity of 500 mAh g^{-1}. The full cell has enhanced safety content, due to the replacement of the lithium metal anode by suitable intercalation electrode, and shows a theoretical energy density as high as 1000 Wh kg^{-1} at high current rate of 1 C. The remarkable safety level, low materials cost, and high practical energy density, expected to exceed 300 Wh kg^{-1}, suggest the battery reported is a suitable energy storage system for future applications.

1. Introduction

Recently, increasing consumption of fossil fuels, atmosphere pollution and consequent climate changes focused renewed attention on renewable energy production systems. Indeed, the discontinuity of these systems and, more recently, the emerging market of the electric vehicles triggered the development of advanced energy storage systems. In this respect, lithium batteries (LIBs) appeared the most promising among the various candidates due to their high theoretical energy and long calendar life.[1] However, the severe targets of the electric vehicle market, as well as the need for decreasing cost of side storage in renewable energy plants, so far required new systems characterized by higher energy density and lower economic impact. Lithium–sulfur battery has high theoretical energy density, i.e., of about 2600 Wh kg^{-1}, and, contemporary, very low cost and earth abundance of the cathode material, hence it is considered the most promising system to meet the emerging market requirements.[2–7] However, the use of sulfur in lithium batteries is still hindered by several issues, preventing a practical application, such as the insulator nature of the cathode, the volume changes during operation and the high solubility of reaction intermediates (e.g., polysulfides) in conventional organic solvents.[8] Lithium sulfur electrochemical process is a multistep reaction involving the initial formation of the highly soluble Li_2S_8 and final precipitation of Li_2S, with an overall capacity of 1675 mAh g^{-1} vs. sulfur mass.[9] The dissolved polysulfide may migrate through the electrolyte from the sulfur cathode to the lithium metal anode, thus leading to a shuttle reaction, an increasing polarization, and a final capacity fading.[10,11] Several researches, involving both the electrodes and the electrolyte, have been devoted to the lithium–sulfur battery in order to mitigate the shuttle reaction and the cathode dissolution. Cathode optimization, mainly focused on sulfur impregnation in modified carbons or functionalized graphene, has been reported as efficient strategy to enhance the electronic conductivity and the cycling stability.[12–15] Ether-based electrolytes, such as tetraethylene glycol dimethyl ether (TEGDME)[8,10,16] and 1,3 dioxolane (DOL) dimethoxyethane (DME), have been selected as suitable media in alternative to conventional carbonate solutions.[17–19] Recent studies demonstrated the positive effect of electrolyte-additives, such as $LiNO_3$, in inhibiting the polysulfide shuttle reaction, due to the formation of a stable layer at the lithium anode surface, thus leading to a remarkable enhancement of the lithium–sulfur cell performance.[18–21] Further studies evidenced that the dissolution of a selected polysulfide, of various nature and concentration, into the electrolyte may efficiently stabilize the sulfur cathode by mass and electrochemical buffer effect.[22–25] A relevant issue affecting the lithium sulfur cell in its conventional configuration is represented by the use of a lithium metal anode that is characterized by safety issues, associated to possible dendrite formation, short circuit, and cell thermal runway. Previous papers demonstrated the possible replacement of lithium metal by Li-alloying materials in an efficient lithium-ion sulfur cell configuration.[3,16,26–28] In this work we report a metal-free, full lithium-ion sulfur battery using graphite-based, intercalation anode, and sulfur–carbon cathode, benefitting by the contemporary positive effect of two additives, i.e., Li_2S_8 and $LiNO_3$

Dr. M. Agostini, Dr. J. Hassoun
Department of Chemistry
University of Rome Sapienza
00185 Rome, Italy
E-mail: jusef.hassoun@uniroma1.it
Prof. B. Scrosati
Istituto Italiano di Tecnologia
16163 Genova, Italy
E-mail: bruno.scrosati@gmail.com

DOI: 10.1002/aenm.201500481

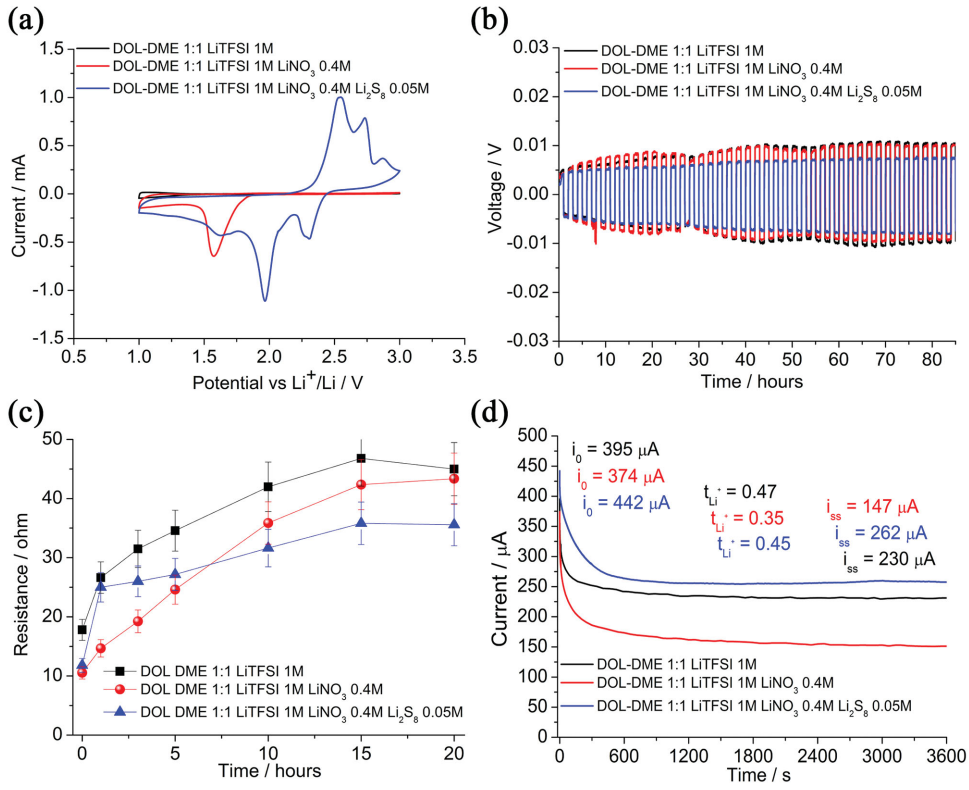

Figure 1. Electrochemical characterization of the DOL-DME (1:1, v/v), 1 M LiTFSI (black), 0.4 M $LiNO_3$-added (red), and 0.4 M $LiNO_3$–0.05 M Li_2S_8-added (blue) electrolytes. a) Cyclic voltammetry performed using a scan rate of 0.1 mV s^{-1} versus Li^+/Li; b) lithium deposition–stripping overvoltage in lithium symmetrical cell using a current of 0.1 mA cm^{-2}; c) time evolution of the lithium symmetrical cell resistance; and d) current–time evolution of the lithium symmetric cells following a DC polarization of 10 mV and, in inset, corresponding t^+ number calculated. Room temperature (25 °C).

dissolved in a DOL-DME solvent. The cell operates at about 2 V and delivers a capacity as high as 500 mAh g^{-1} vs. sulfur cathode mass with extended stability, limited polarization, and high charge–discharge efficiency, i.e., a relevant performance suitable for the development of a safe, high energy storage system.

2. Results and Discussion

Figure 1 reports the comparison of the electrochemical characteristics of the bare DOL-DME-LiTFSI electrolyte, and the solutions added by $LiNO_3$ and by Li_2S_8 in terms of cyclic voltammetry in lithium cells using Super P carbon working electrode (a), lithium stripping–deposition polarization in symmetric Li/Li cells (b), stability against lithium metal (c), and Li-transference number (d). The cyclic voltammetry performed using the pristine solution (Figure 1a, black line) shows a flat profile and absence of relevant peaks. The presence of $LiNO_3$ within the solutions (Figure 1a, red and blue lines) reveals a reduction peak at around 1.5 V, associated to the irreversible reaction of the $LiNO_3$.[29] The reversible electrochemical reduction of the polysulfide appears for the final solution, added by both $LiNO_3$ and Li_2S_8 (Figure 1a, blue line), at around 2.4 and 2.0 V versus Li^+/Li in discharge, while the following oxidation occurs above 2.6 V in charge.[10] The Li-stripping-deposition tests reported in Figure 1b evidence a polarization limited to few mV and a stable trend for several cycles, thus suggesting the compatibility of the lithium with the selected electrolytes. The suitability of the electrolytes in lithium cell is further confirmed by Figure 1c, reporting the time evolution of the interphase resistance. The figure reveals a slight resistance growth during the initial 10 h of test, associated to the solid electrolyte interphase (SEI) film formation upon chemical reaction of lithium with the electrolyte, and a following stabilization due to the consolidation of the SEI.[10,24] The same figure evidences that the solution added by $LiNO_3$ and Li_2S_8, selected as the preferred electrolyte media for sulfur cell application, is characterized by the lowest cell resistance, due to the beneficial effect of the two additives. The lithium transference number (t_{Li+}) of the electrolytes has been calculated according to the Bruce–Vincent equation.[30] Figure 1d reports the comparison of the current–time curves of the symmetrical lithium cell assembled using the three electrolytes and polarized at 10 mV (the corresponding impedance responses used for t_{Li+} determination are reported in the Supporting Information, Figure S1). The t_{Li+}, calculated to be of 0.47 for the pristine electrolyte in agreement with literature data,[31] decreases to 0.35 by addition of $LiNO_3$ salt due to the increased ionic force of the solution, and rises back up to 0.45 by Li_2S_8 addition due to its possible contribution to the lithium ion mobility, thus suggesting that $LiNO_3$ and Li_2S_8 finally affect the lithium transference number.

The sulfur–carbon electrode employed in this work, i.e., a sulfur-mesophase carbon micro beads (S-MCMB) composite, has micrometric morphology and S-loading of about 50%,

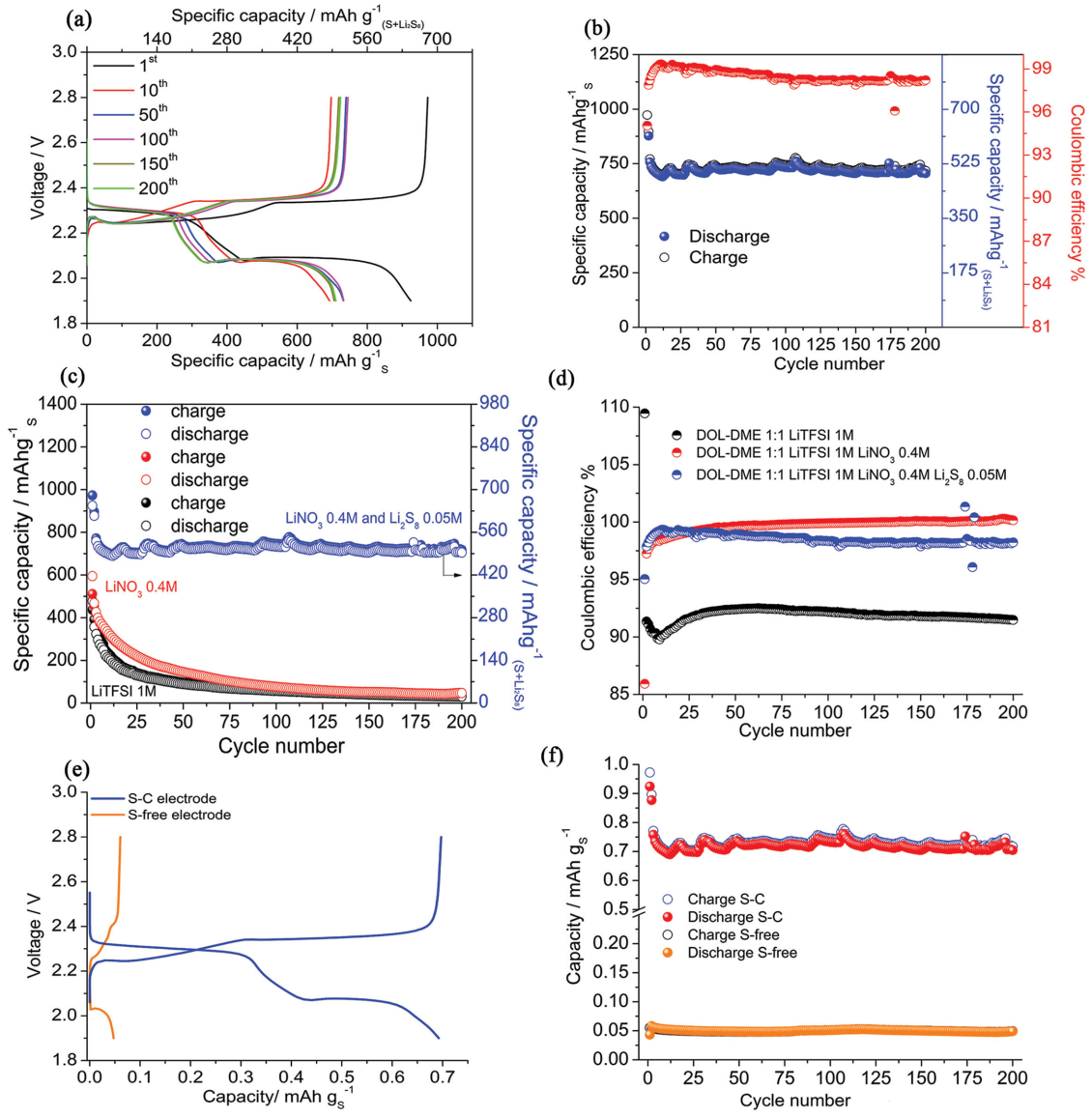

Figure 2. a) Voltage profiles and b) cycling behavior (with corresponding coulombic efficiency reported by red circles in right side) of a Li/ DOL-DME (1:1, v/v), 1 M LiTFSI, 0.4 M $LiNO_3$, 0.05 M Li_2S_8/S–C cell. Comparison of the c) cycling behavior and d) coulombic efficiency of the Li/S–C cells using the three electrolytes: bare DOL DME 1:1 LiTFSI 1 M, 0.4 M $LiNO_3$-added, and 0.4 M $LiNO_3$–0.05 M Li_2S_8-added electrolyte; specific capacity versus total sulfur amount on the right axis. e) Cycling behavior and f) corresponding voltage profile of a lithium cell using a sulfur-free carbon electrode (MCMB, Super P, and PVdF 6020 in the 8:1:1 weight ratio) in comparison to a cell using the S–C electrode. Voltage range 1.9–2.8V, current of 1.675 A g^{-1} (corresponding to 1 C of sulfur electrode). Room temperature (25 °C).

evidenced by scanning electron microscopy (SEM) and thermogravimetric analysis (TGA) reported in the Supporting Information, Figure S2a,b, respectively.[32] This electrode configuration, characterized by remarkable solubility during operation in lithium cell using bare electrolytes, shows significant improvements, both in terms of cycling stability and coulombic efficiency, in lithium cell using polysulfide-added electrolytes.[24] **Figure 2**a,b reports the Li/S cell performances in terms of voltage profile and cycling behavior using the electrolyte added by both $LiNO_3$ and Li_2S_8. The cell, cycled using a current as high as 1.675 A g^{-1} (1 C), shows a capacity of 900 mAh g^{-1} and an efficiency of 95% in the 1st cycle. During the following cycles, the capacity decreases to a value of about 750 mAh g^{-1} stable for over 200 cycles, with an average working voltage of 2.2 V and an efficiency approaching 99% (Figure 2a,b). The lithium cell using the bare electrolyte shows remarkable capacity fading due to dissolution of the sulfur electrode (Figure 2c) and a low coulombic efficiency (Figure 2d) due to the shuttle reaction of the dissolved cathode. The efficiency rises by $LiNO_3$ addition, due to the formation of a favorable SEI film, however the cell appears still affected by capacity fading. Furthermore, the contemporary effect of the two additives, i.e., $LiNO_3$ and Li_2S_8, well stabilizes the cell capacity and enhances the coulombic efficiency to value close to 100%. Indeed, the specific capacity delivered by the

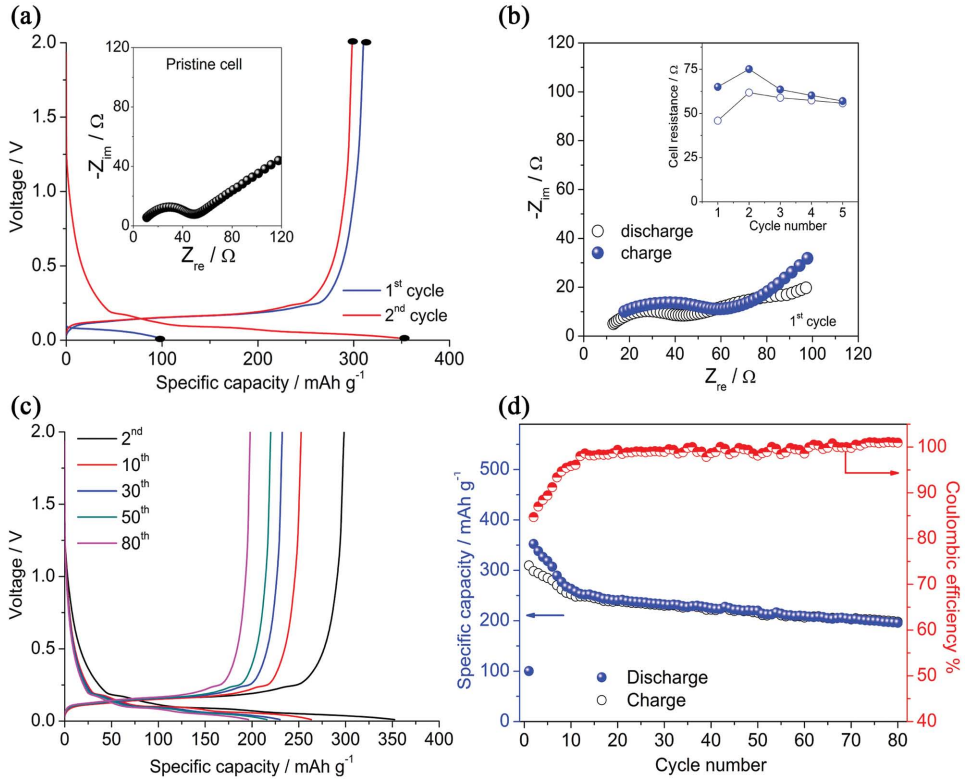

Figure 3. a) Voltage profile of the 1st and 2nd cycles of the Li/ DOL-DME (1:1, v/v), 1 M LiTFSI, 0.4 M $LiNO_3$, 0.05 M Li_2S_8/graphite lithium-cell cycled using a current of 200 mA g^{-1} within voltage ranging from 0.01 to 2.0 V voltage range and, in inset, impedance Nyquist plot of the cell at the pristine state. b) Nyquist plots of the cell upon the first discharge (empty black circles) and the following charge (plain blue circles) and, in inset, evolution of the cell resistance during cycling. c) Voltage profiles and d) cycling behavior (with corresponding coulombic efficiency reported by red circles in right side) of the cell upon prolonged cycling. Room temperature (25 °C).

Li/S cell using the modified electrolyte is about 750 mAh g^{-1} as referred to the sulfur mass in the electrode that is reduced to 525 mAh g^{-1} considering the overall S mass, including dissolved polysulfide (right-side Y axis). In this work, the Li–S cell capacity has been referred to the sulfur mass in the cathode neglecting the direct participation of Li_2S_8 dissolved within the electrolyte to the electrochemical process. Indeed, this process has been directly investigated by the cycling test employing a sulfur-free carbon electrode, i.e., formed by MCMB, and Li_2S_8-added electrolyte. The response of this cell in terms of voltage profile (Figure 2e) and cycling behavior (Figure 2f), in comparison to the corresponding test in lithium cell using the sulfur carbon electrode, demonstrates a minor contribution of the polysulfide to the overall Li/S cell capacity, i.e., of about 7%. Indeed, within our cell configuration, the limited amount of dissolved Li_2S_8 mainly acts as mass buffer leading to cycling stabilization, while $LiNO_3$ salt increases the cell efficiency.

A graphite-based anode has been characterized in lithium cell using the DOL DME 1:1 LiTFSI 1 M, $LiNO_3$ 0.4 M, Li_2S_8 0.05 M electrolyte solution in order to verify its suitability for application in full, lithium-ion sulfur cell. Prior to test, the graphite electrode has been fully prelithiated by direct contacting with a lithium foil wet by LP30 electrolyte, as reported in previous paper.[27] The interphase of the lithiated graphite electrode has been studied in lithium cell by using electrochemical impedance spectroscopy (EIS). **Figure 3**a reports the voltage profile of the 1st and 2nd cycles of the Li/ DOL-DME (1:1, v/v), 1 M LiTFSI, 0.4 M $LiNO_3$, 0.05 M Li_2S_8/ graphite cell studied using a current of 200 mA g^{-1} within voltage ranging from 0.01 to 2.0 V. The figure evidences a delivered capacity of about 100 mAh g^{-1} during the first discharge, increasing to about 310 mAh g^{-1} during the following charge. This trend is due to the activation process (see the Experimental Section) that leads to a partial lithium insertion into the electrode structure, reduction of the pristine cell working voltage as well as to the formation of a stable SEI film thus avoiding further reaction of the electrode with the electrolyte components, e.g., Li_2S_8 and $LiNO_3$. Hence, the formation of a passivation layer kinetically protects the graphite electrode surface. Indeed, the inset of Figure 3a, reporting the impedance Nyquist plot of the cell at the pristine state, demonstrates a low cell resistance, i.e., limited to about 45 Ω. Furthermore, the Nyquist plots of the cell upon the first discharge (empty black circles) and the following charge (plain blue circles) reported in Figure 3b and the evolution of the cell resistance during cycling (reported in inset) further confirm the stability of the SEI film formed by prelithiation of graphite electrode prior to cycle. The slight changes observed in Figure 3b may be most likely attributed to minor changes in SEI film composition by cycling in DOL-DME-LiTFSI-$LiNO_3$-Li_2S_8

electrolyte. Figure 3c, reporting the voltage profiles of the lithiated graphite electrode, reveals an average working voltage of about 0.2 V versus Li^+/Li, while the cycling behavior of Figure 3d evidences a decay during the initial ten cycles, followed by a stabilization of the capacity at about 240 mAh g^{-1}, i.e., about 65% of the expected theoretical value (370 mAh g^{-1}). The capacity decay, and the low initial cell efficiency, during the initial cycles may be attributed to possible slight SEI film modification and structural organization of the electrode surface in presence of the additional salts, i.e., $LiNO_3$ and Li_2S_8, required for an optimal operation of the sulfur cathode side.[10,24,27,29] However, the stable trend of the cycling test during the following cycles is considered convincing proof, suggesting the suitability of the lithiated-graphite electrode in full Li-ion sulfur cell configuration.

Figure 4 reports the electrochemical response of the Li-ion sulfur cell formed by coupling the sulfur–carbon cathode, the prelithiated graphite anode and the selected electrolyte solution, i.e., added by $LiNO_3$ and Li_2S_8, using a current–rate as high as of 1675 mA g^{-1} (corresponding to 1 C). During the first cycle, the discharge of about 1000 mAh g^{-1} is not completely reversed upon the following charge process, due to the above observed initial irreversible trend of the graphite electrode, thus leading to a coulombic efficiency higher than 100% (i.e., calculated as percentage of the discharge capacity in respect to charge capacity). Furthermore, the cell shows capacity decay during the first ten cycles, as most likely ascribed to the anode stabilization already observed in the cycling test reported in Figure 3. During the following cycles a stable capacity of about 500 mAh g^{-1} (in respect to S in the cathode), a working voltage of about 2 V, a high coulombic efficiency, and a limited polarization are shown. The steady state voltage profile of Figure 4a reflects the reversible electrochemical reaction of sulfur with lithiated graphite

$$S8 + 16LiC_6 = 8Li_2S + 16C_6$$

This notable performance suggests a stable energy density, theoretically of about 1000 Wh kg^{-1} referred to the sulfur loaded in the cathode that is a value much higher than that offered by the commercial Li-ion battery.[1] The cell has additional bonus: the extremely reduced cost of the component materials, i.e., sulfur and graphite, and the high safety content.

3. Conclusions

The lithium-ion sulfur cell here reported shows enhanced performances due to the beneficial addition of $LiNO_3$ and Li_2S_8 to the DOL-DME-LiTFSI solution used as the electrolyte media. The two additives properly suppress the polysulfide shuttle reaction and buffer the sulfur cathode dissolution within the electrolyte, thus leading to optimized electrochemical process. Furthermore, the replacement of the lithium metal by a carbon anode based on intercalation process well increases the cell safety. The excellent performances of the full cell, in terms of delivered capacity, current rate, energy density, and cycling life, confirm the suitability of the system here proposed for high energy applications.

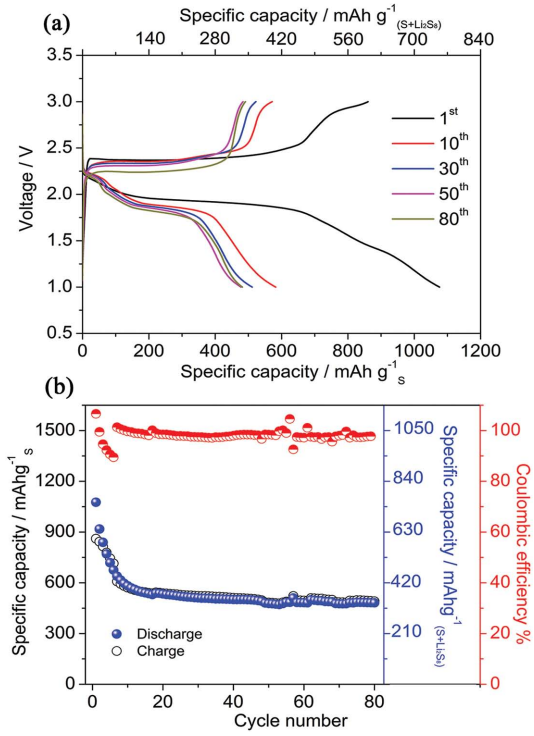

Figure 4. a) Voltage profile at the 1st, 10th, 30th, 50th, 80th cycle and b) cycling behavior (with corresponding coulombic efficiency reported by red circles in right side) of the LiC_6/ DOL-DME (1:1, v/v), 1 M LiTFSI, 0.4 M $LiNO_3$, 0.05 M Li_2S_8/S–C lithium-ion sulfur cell performed at a current of 1.675 A g^{-1} (1 C) within 1.0–3.0 V voltage range. Room temperature (25 °C).

4. Experimental Section

Electrodes Preparation: The cathode material was prepared by melting sulfur (Aldrich 99.9%) at 135 °C and then mixing it with MCMB (mesophase carbon micro beads, Osaka gas) with a 1:1 weight ratio using a procedure reported in a previous paper.[32] Following, the mixture was refined for 2 h by using the high energy mechanical milling (HEMM). The sulfur–carbon electrode morphology was investigated by scanning electron microscopy using a Phenom-FEI instrument. The S–C thin film electrode was prepared by mixing the active material powder with Super P carbon (conducting agent, Timcal) and polyvinylidene fluoride (PVdF 6020, binder, Solvay) in a weight ratio of 8:1:1 using *N*-methyl pirrolidone (NMP). The resulting slurry was then cast on an Al foil of approximately 40 μm thickness to achieve a sulfur loading of about 1.3 mg cm^{-2}. The electrodes were dried at 50 °C under vacuum to remove residual solvent, prior to be used in lithium cells. The anode was prepared by mixing MCMB powder with Super P carbon (conducting agent, Timcal) and PVdF (6020, binder, Solvay) in the weight ratio of 8:1:1 and dissolving the mixture in NMP (Aldrich). The resulting slurry was plated on a Cu foil, with a final graphite loading of 5 mg cm^{-2}. The electrodes were dried at 100 °C under vacuum, prior to be used in lithium cells.

Electrolytes Preparation: The bare, additive-free electrolyte was prepared in argon-filled glove box by dissolving 1 mol of LiTFSI (Aldrich) in 1 L of DME (Dimethoxyethane, Aldrich)/DOL (Dioxolane, Aldrich) with a 1:1 volume ratio. A second test-solution was prepared by adding to 1 L of the bare solution 0.4 mol of $LiNO_3$. The final, polysulfide-containing electrolyte was prepared by following two steps: (i) mixing lithium metal and elemental sulfur in a molar ratio of 2:8 in DME/DOL solution to reach a Li_2S_8 concentration of 0.05 mol L^{-1}, and heating at

80 °C for 12 h, until a red-color solution is obtained, (ii) dissolving 1 mol of LiTFSI and 0.4 mol of $LiNO_3$ to 1 L of DME-DOL-Li_2S_8 solution above described to reach the following electrolyte configuration: 1 M LiTFSI, 0.4 M $LiNO_3$, 0.05 M Li_2S_8 in DME/DOL (1:1 = v/v).

Electrochemical Measurements: The lithium–electrolyte interphase resistance was determined using a lithium–lithium symmetric 2032 coin type cell by electrochemical impedance spectroscopy applying a 10 mV AC amplitude signal within 500 kHz–10 mHz frequency range. The determination of lithium transference numbers were obtained by using the Bruce–Vincent[30] method that combines AC and DC polarization to a Li/Li symmetrical cell using the selected electrolyte. The formula used for the lithium transference number determination was $t_{Li+} = I_{ss}(\Delta V - R_0 I_0)/I_0(\Delta V - R_{ss} I_{ss})$, where I_0 is the initial current, I_{ss} the steady state current, ΔV the applied voltage, and R_0 and R_{ss} are resistances before and after dc polarization, respectively. The applied DC signal was of 10 mV while the EIS was performed before and after polarization within 500 kHz–10 mHz frequency range, using 10 mV amplitude AC pulses. The cyclic voltammetry (CV) tests were performed using a three electrode polypropylene T-cell, with lithium foil as reference and counter electrode and carbon Super P (Super P, PVdF 6020 8:2 on Al foil) as working electrode. The CV tests were run with a scan rate of 0.1 mV s^{-1}, within 1–3 V voltage range. The resistance of the films formed by the electrolytes was evaluated by using EIS technique on a Li/ DOL-DME (1:1, v/v), 1 M LiTFSI, 0.4 M $LiNO_3$, 0.05 M Li_2S_8/Li cell. The measurement was performed within a 500 kHz–10 mHz frequency range, by applying a 10 mV amplitude AC pulse from pristine condition and upon 20 h of aging after cell assembling. The interphase resistance value was evaluated by nonlinear least squares (NLLS) fit of the high-frequency semicircles related to the film formation process. All the above tests were performed using VMP3 Biologic instrument. The galvanostatic tests were carried out in a 2032 coin-type cell by using a Maccor Series 4000 Battery Test System (Maccor, Inc.). Electrochemical charge–discharge study in lithium cell was performed within 1.9–2.8 V at a current of 1.675 A g^{-1} (1 C) for the S–C electrode and within 0.01–2.0 V at a current of 200 mA g^{-1} for the graphite electrode. The lithium ion full cell was assembled by coupling the S–C cathode and the graphite anode. Prior to the cell testing, the graphite anode was prelithiated by contacting with a lithium foil wet by ethylene carbonate:dimethyl carbonate (EC:DMC 1:1, v:v), $LiPF_6$ (1 M), and following rinsing by dimethyl carbonate (DMC, Aldrich, 99%) as reported in previous paper.[27] The graphite/lithium interphase was investigated by coupling EIS and galvanostatic cycling (GC) techniques. The EIS was performed in 500 kHz–10 mHz frequency range, using 10 mV amplitude AC pulses, in the pristine state of the cell and after discharge and charge process, from 1st to 5th cycles. Before the test in lithium cell the graphite electrode was pretreated by Li-metal as above reported. GC was performed in lithium cell within 0.01 and 2.0 V at a current of 200 mA g^{-1}. The full cell was balanced by selecting 1:4 cathode to anode mass ratio. The lithium ion cell was cycled at 1 C current rate (1.675 A g^{-1}), referring to the sulfur–cathode active mass, within 1–3V voltage range. The cell capacity was referred both to sulfur active mass (about 1 mg) and to the overall sulfur mass (S weight in the cathode and in the electrolyte). An Advantec glass fiber was used as separator and soaked by 40 µL of the selected electrolyte solution, with a Li_2S_8 content of about 0.5 mg (corresponding to 0.45 mg of sulfur, see results and discussion of Figure 2 for clarification).

Supporting Information

Supporting Information is available from the Wiley Online Library or from the author.

Received: March 9, 2015
Revised: May 20, 2015
Published online: June 22, 2015

[1] J.-M. Tarascon, M. Armand, *Nature* **2001**, *414*, 359.
[2] E. Peled, A. Gorenshtein, M. L. Sega, Y. Sternberg, *J. Power Sources* **1989**, *26*, 269.
[3] J. Hassoun, B. Scrosati, *Angew. Chem. Int. Ed.* **2010**, *49*, 2371.
[4] L. F. Nazar, M. Cuisinier, Q. Pang, *MRS Bull.* **2014**, *39*, 436.
[5] R. D. Rauh, K. M. Abraham, G. F. Pearson, J. K. Surprenant, S. B. Brummer, *J. Electrochem. Soc.* **1979**, *126*, 523.
[6] N. Jayaprakash, J. Shen, S.-S. Moganty, A. Corona, L.-A. Archer, *Angew. Chem. Int. Ed.* **2011**, *50*, 5904.
[7] D. Bresser, S. Passerini, B. Scrosati, *Chem. Commun.* **2013**, *49*, 10545.
[8] J. Hassoun, M. Agostini, A. Latini, S. Panero, Y.-K. Sun, B. Scrosati, *J. Electrochem. Soc.* **2012**, *159*, A1.
[9] S.-H. Chung, A. Manthiram, *J. Power Sources* **2013**, *107*, 569.
[10] M. Agostini, D.-J. Lee, B. Scrosati, Y.-K. Sun, J. Hassoun, *J. Power Sources* **2014**, *265*, 14.
[11] Y.-V. Mikhaylik, J. R. Akridge, *J. Electrochem. Soc.* **2004**, *151*, A1969.
[12] X. L. Ji, K. T. Lee, L. F. Nazar, *Nat. Mater.* **2009**, *8*, 500.
[13] J.-H. Kim, D.-J. Lee, H.-G. Jung, Y.-K. Sun, J. Hassoun, B. Scrosati, *Adv. Funct. Mater.* **2013**, *23*, 1076.
[14] G. He, X. Ji, L. Nazar, *Energy Environ. Sci.* **2011**, *4*, 2878.
[15] H. Wang, Y. Yang, Y. Liang, J. T. Robinson, Y. Li, A. Jackson, Y. Cui, *Nano Lett.* **2011**, *11*, 2644.
[16] M. Agostini, J. Hassoun, J. Liu, M. Jeong, H. Nara, T. Momma, T. Osaka, Y.-K. Sun, B. Scrosati, *ACS Appl. Mater. Interfaces* **2014**, *6*, 10924.
[17] Y. Mikhaylik, I. Kovalev, R. Schock, K. Kumaresan, J. Xu, J. Affinito, *ECS Trans.* **2010**, *25*, 23.
[18] S. Xiong, K. Xie, Y. Diao, X. Hong, *Electrochim. Acta* **2012**, *83*, 78.
[19] S.-S. Zhang, *J. Power Sources* **2013**, *231*, 153.
[20] D. Aurbach, E. Pollak, R. Elazari, G. Salitra, C. S. Kelley, J. Affinito, *J. Electrochem. Soc.* **2009**, *156*, A694.
[21] C. Barchasz, J. C. Leprêtre, F. Alloin, S. Patoux, *J. Power Sources* **2012**, *199*, 322.
[22] R. Demir-Cakan, M. Morcrette, A. Gangulibabu, R. Gueguen, R. Dedryvere, J.-M. Tarascon, *Energy Environ. Sci.* **2013**, *6*, 176.
[23] S.-S. Zhang, J. A. Read, *J. Power Sources* **2012**, *200*, 77.
[24] D.-J. Lee, M. Agostini, J.-W. Park, Y.-K. Sun, J. Hassoun, B. Scrosati, *ChemSusChem* **2013**, *6*, 2245.
[25] S. Chen, F. Dai, M. L. Gordin, D. Wang, *RSC Adv.* **2013**, *3*, 3540.
[26] M. Agostini, J. Hassoun, *Sci. Rep.* **2015**, *5*, 7591.
[27] J. Hassoun, J.-H. Kim, D.-J. Lee, H.-G. Jung, S.-M. Lee, Y.-K. Sun, B. Scrosati, *J. Power Sources* **2012**, *202*, 308.
[28] Y. Yang, M. T. McDowell, A. Jackson, J. J. Cha, S. S. Hong, Y. Cui, *Nano Lett.* **2010**, *10*, 1486.
[29] D. Aurbach, *J. Power Sources* **2000**, *89*, 206.
[30] P. Bruce, G. Evans, C. A. Vincent, *Solid State Ion.* **1988**, *28*, 918.
[31] L. Suo, Y. S. Hu, H. Li, M. Armand, L. Chen, *Nat. Commun.* **2013**, *4*, 1481.
[32] M. Agostini, Y. Ahiara, T. Yamada, B. Scrosati, J. Hassoun, *Solid State Ion.* **2013**, *244*, 48.